nature chemistry

SUPPLEMENTARY INFORMATION

https://doi.org/10.1038/s41557-018-0164-y

In the format provided by the authors and unedited.

Heteromultivalent peptide recognition by co-assembly of cyclodextrin and calixarene amphiphiles enables inhibition of amyloid fibrillation

Zhe Xu[1,2], Shaorui Jia[3], Wei Wang[1], Zhi Yuan[1], Bart Jan Ravoo[2*] and Dong-Sheng Guo[1,4*]

[1]College of Chemistry, State Key Laboratory of Elemento-Organic Chemistry, Key Laboratory of Functional Polymer Materials, Ministry of Education, Nankai University, Tianjin, China. [2]Organic Chemistry Institute and Center for Soft Nanoscience (SoN), Westfälische Wilhelms-Universität Münster, Münster, Germany. [3]College of Life Sciences, Key Laboratory of Bioactive Materials, Ministry of Education, Nankai University, Tianjin, China. [4]Collaborative Innovation Center of Chemical Science and Engineering, Nankai University, Tianjin, China. *e-mail: b.j.ravoo@uni-muenster.de; dshguo@nankai.edu.cn

Supporting Information

for

Heteromultivalent Peptide Recognition by Co-Assembly of Cyclodextrin and Calixarene Amphiphiles Enables Inhibition of Amyloid Fibrillation

Zhe Xu,[1,2] Shao-Rui Jia,[3] Wei Wang,[1] Zhi Yuan,[1] Bart Jan Ravoo *[2] and Dong-Sheng Guo*[1,4]

[1] *College of Chemistry, State Key Laboratory of Elemento-Organic Chemistry, Key Laboratory of Functional Polymer Materials, Ministry of Education, Nankai University, Tianjin 300071, P. R. China E-mail:* dshguo@nankai.edu.cn.

[2] *Organic Chemistry Institute and Center for Soft Nanoscience (SoN), Westfälische Wilhelms-Universität Münster, Corrensstrasse 40, 48149 Münster, Germany E-mail:* b.j.ravoo@uni-muenster.de.

[3] *College of Life Sciences, Key Laboratory of Bioactive Materials, Ministry of Education, Nankai University, Tianjin 300071, P. R. China.*

[4] *Collaborative Innovation Center of Chemical Science and Engineering, Nankai University, Tianjin 300071, P. R. China.*

Table of contents

1. Materials and methods·····1-2

2. Characterization of the CD–CA co-assembly·····3-5

3. Results and experimental raw data supporting heteromultivalency ·····6-15

3.1 Binding between **LCG** and the **CD–CA** co-assembly or the **CA** assembly ·····6-7

3.2 Binding of calixarene with lysine (**K**) and arginine (**R**) ·····7-8

3.3 Binding of model peptides with the **CA** assembly, **CD** assembly, **CD–CA** co-assembly and the simple mixture ·····8-15

4. Characterization of the effects of the CD–CA co-assembly on Aβ_{42} ·····16-17

4.1 Binding between **Aβ_{42}** and the **CD–CA** co-assembly ····· 16-17

4.2 Effects of the **CD–CA** co-assembly on dissolving **Aβ_{42}** fibrils ·····17

5. References·····18

1. Materials and methods

Materials. All reagents and solvents were commercially available and used as received unless otherwise specified purification. Thioflavin T (**ThT**), diphenylhexatriene (**DPH**) and lucigenin (**LCG**) were purchased from Sigma-Aldrich. 2-(4-phenylboronic acid)-1-pyrenemethamide (**PB**), 5,11,17,23,29-Pentacarboxylic acid-31,32,33,34,35-*n*-dodecyloxy calix[5]arene (**CA**) and amphiphilic β-cyclodextrin (**CD**) were synthesized and purified according to the literature procedures.[1-4] All model peptides and amyloid β-peptide (**Aβ_{42}**) (>95%) were purchased from GL Biochem (Shanghai, China) as a lyophilized powder. β-Cyclodextrin was purchased from Sigma-Aldrich and sulfonatocalix[4]arene (**SC4A**) was synthesized and purified according to the literature procedures.[5] Hexafluoro-2-propanol (HFIP), 3-(4,5-dimethylthiazol-2-yl)-2,5-diphenyltetrazolium bromide (MTT), and dimethyl sulfoxide (DMSO) were purchased from Sigma (St. Louis, MO, USA). Dulbecco's modified Eagle medium (DMEM) and fetal bovine serum were obtained from GIBCO (Grand Island, NY, USA). The highly differentiated rat pheochromocytoma cell line (PC-12) was purchased from Cell Bank of Chinese Academy of Science. The 4-(2-hydroxyethyl)-1-piperazineethanesulfonic acid (HEPES) buffer solution (10 mM) of pH 8.0 was prepared by dissolving 2.383 g of HEPES in approx. 900 ml of double-distilled water, titration to pH 8.0 at room temperature of 25 °C with NaOH and dilution to a volume of 1000 ml with double-distilled water. The 10 mM phosphate buffer solution (PBS) of pH 7.4 was prepared by dissolving 1.56 g of $NaH_2PO_4{\cdot}2H_2O$ in approx. 900 ml of double-distilled water, titration to pH 7.4 at room temperature of 25 °C with NaOH and dilution to a volume of 1000 ml with double-distilled water. The pH value of all the buffer solutions were verified on a pH-meter calibrated with two standard buffer solutions

Scanning electron microscopy (SEM). SEM images were recorded on a Hitachi S-3500N scanning electron microscope. The samples for SEM measurements were prepared by dropping the solution onto a coverslip, followed by evaporating the liquid in air.

Differential scanning calorimetry (DSC) measurements. DSC measurements were carried out on a DSC Q100 (TA Instruments). The co-assembly solutions (50 μL) were sealed in pressure-resistant DSC cups and scanned against a reference cup of HEPES buffer (pH = 8.0, 10 mM). The samples were equilibrated at 5 °C, then heated to 80 °C at 1 °C/min. After cooling the sample to room temperature, the measurements were repeated at least five times.

Fluorescence spectroscopy. Steady-state fluorescence spectra were recorded in 1 mL low-volume disposable PMMA cuvettes (Brand GmbH & CO KG, Wertheim) on a JASCO FP 6500 and a

conventional quartz cell (light path 10 mm) on a Varian Cary Eclipse equipped with a Varian Cary single-cell peltier accessory to control temperature.

DPH fluorescence polarization. Measurements were made using an excitation wavelength of 355 nm, an emission wavelength of 430 nm, 5 nm excitation and emission slits, and FP110 film polarizers. To incorporate **DPH** into assembly, a stock solution of 1 mM **DPH** was prepared in tetrahydrofuran, and 3 μl was added to 3 ml of **CD** (100 μM) assembly, **CA** (100 μM) assembly and **CD–CA** (50/50 μM) co-assembly. The sample was mixed vigorously at 80 °C. **CD** (50 μM) assembly direct mixed with **CA** (50 μM) assembly was also measured by incorporate **DPH** in **CD** and **CA** assembly respectively before simply mixed. The cuvette chamber was maintained at the required temperature using a circulating water bath and was allowed to equilibrate for 15-20 min prior to fluorescence measurements. **DPH** polarization was quantified using steady state fluorescence anisotropy measurements calculated according to the literature.[6]

Dynamic light scattering (DLS) and Zeta potential measurements. DLS measurements were examined on a laser light scattering spectrometer (BI-200SM) equipped with a digital correlator (Turbo Corr.) at 636 nm at a scattering angle of 90°. Zeta potential was measured by Zeta PALS + BI-90 instrument (Brookhaven Co. USA).

Transmission electron microscopy (TEM). All experiments were performed by using TEM (FEI, Tecnai G2 F20, U.S.A.). To detect the effect of the inhibitors on **Aβ_{42}** aggregation, TEM was used to observe the peptide morphology. Samples were prepared by placing a 15 μL droplet of sample solution on a carbon support Cu-coated grid for 90 s, and then the excess fluid was wicked away. Subsequently, the samples were negatively stained with 1% tungstophosphoric acid for 90 s, the excess fluid was removed, and the grids were placed in a vacuum drier and dried at room temperature.

2. Characterization of the CD-CA co-assembly

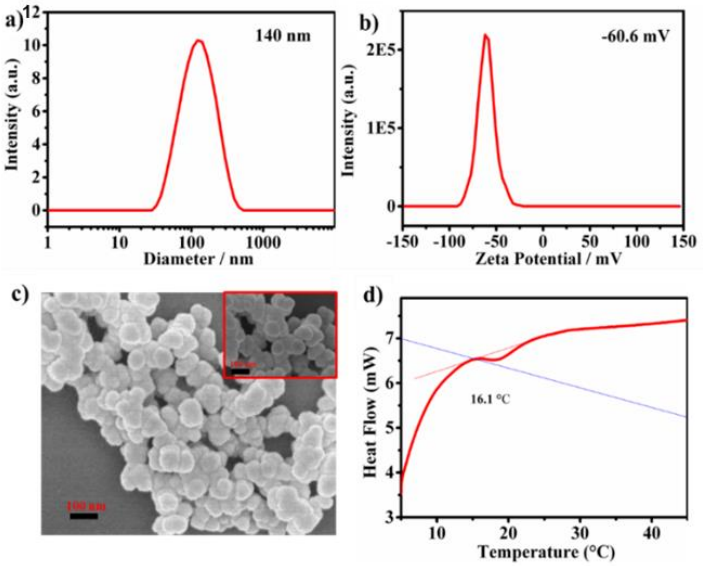

Figure 1. (a) DLS data, (b) Zeta potential, and (c) SEM image of the **CD–CA** co-assembly in 10 mM HEPES buffer (pH = 8.0, [**CA**] = 100 μM, [**CD**] = 100 μM). (d) DSC heating curve for phase transition temperature measurement in 10 mM HEPES buffer (pH = 8.0, [**CA**] = 2.0 mM, [**CD**] = 2.0 mM).

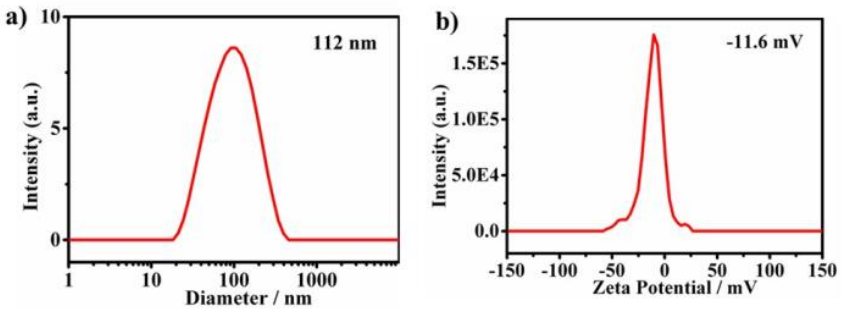

Figure 2. (a) DLS data and (b) Zeta potential of the **CD** assembly in 10 mM HEPES buffer (pH = 8.0, [**CD**] = 100 μM).

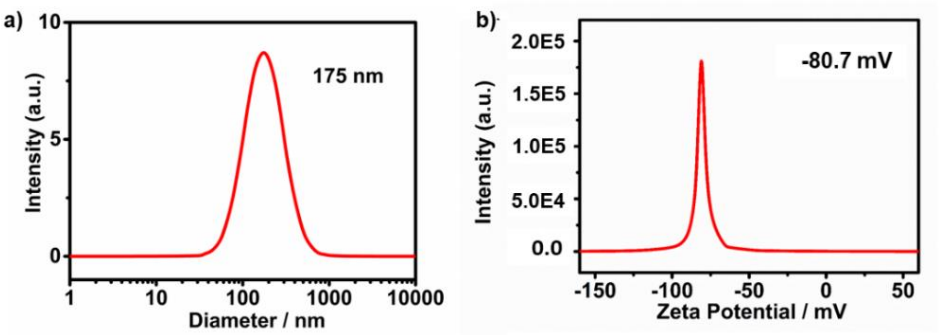

Figure 3. (a) DLS data and (b) Zeta potential of the **CA** assembly in 10 mM HEPES buffer (pH = 8.0, [**CA**] = 100 μM). Note: the **CA** assembly was prepared by using a probe sonicator.

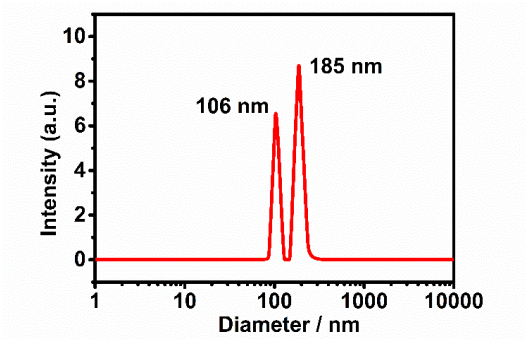

Figure 4. DLS data of the simple mixture of the **CD** and **CA** assemblies in 10 mM HEPES buffer (pH = 8.0, [**CD**] = 100 μM, [**CA**] = 100 μM).

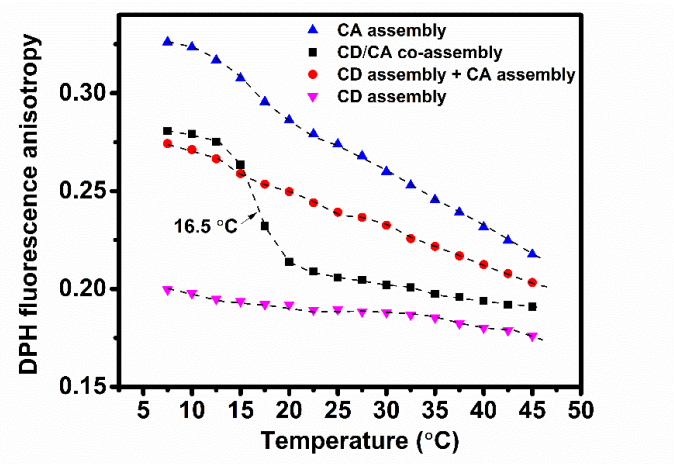

Figure 5. Temperature dependence of the steady-state anisotropy of **DPH** in assembly: the **CD** (100 μM) assembly (▼), the **CA** (100 μM) assembly (▲), the simple mixture of **CD** (50 μM) and **CA** (50

μM) assemblies (●) and the **CD–CA** (50/50 μM) co-assembly (■) in HEPES buffer (10 mM, pH = 8.0).

DPH fluorescence polarization results show the phase transition temperature (T_m) of 16.5 °C for the **CD–CA** co-assembly (Supplementary Fig. 5), In contrast, the **CD** or **CA** assemblies show no apparent T_m in region of 7.5-45°C. For the **CD** assembly, its T_m may be lower than 7.5°C. For the **CA** assembly, it may only have a single phase state presented in the bilayer which causes no T_m can be detected.

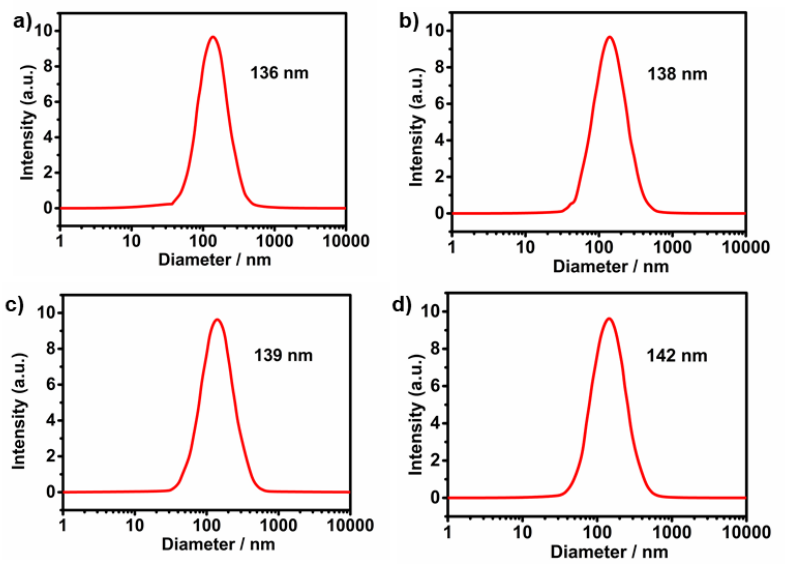

Figure 6. DLS data of (a) the **CD–CA** (1.0/1.0 μM) co-assembly, (b) the **CD–CA** (1.0/1.0 μM) co-assembly after standing for 5 days, (c) the **CD–CA** (20/20 μM) co-assembly and (d) the **CD–CA** (20/20 μM) co-assembly after standing for 5 days in 10 mM HEPES buffer at pH 8.0.

The obtained results show that the size of the **CD–CA** co-assembly is still around 140 nm, which is consistent with the measurement at 100 uM. Moreover, the **CD–CA** co-assembly is stable for at least 5 days.

3. Results and experimental raw data supporting heteromultivalency

3.1 Binding between LCG and the CD–CA co-assembly or the CA assembly

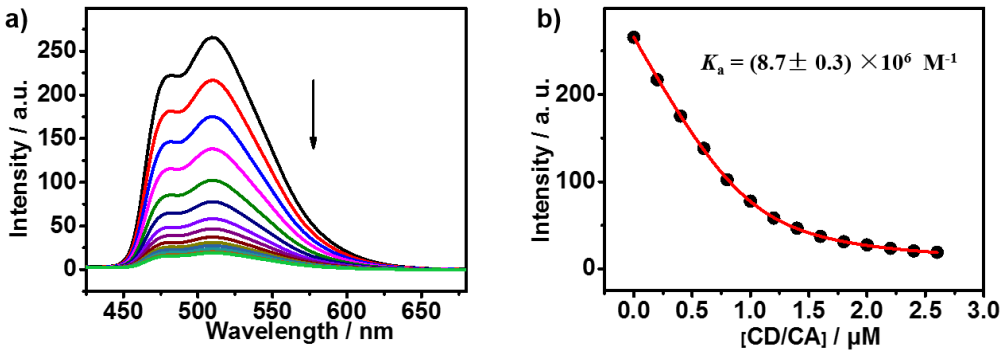

Figure 7. (a) Direct fluorescence titration of **LCG** (1.0 μM) with the **CD–CA** co-assembly in 10 mM HEPES buffer at pH 8.0, λ_{ex} = 365 nm. (b) The associated titration curve at λ_{em} = 510 nm and fit according to a 1:1 binding stoichiometry based on the concentration of the **CA** unit. Data are from n = 3 independent experiments and are presented as mean ± s.e.m..

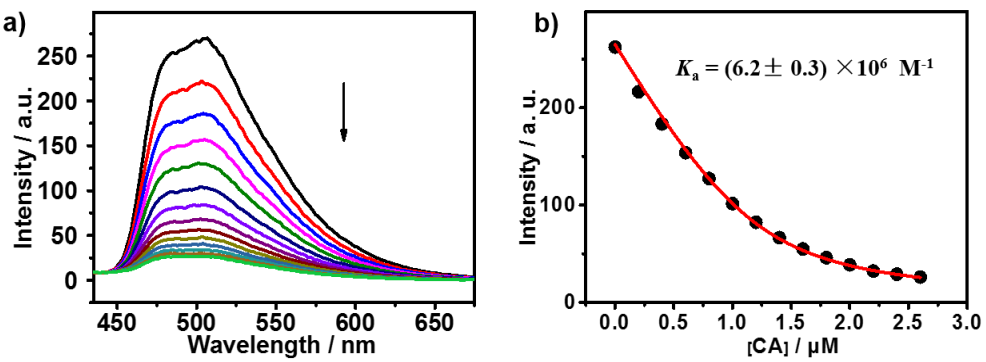

Figure 8. (a) Direct fluorescence titration of **LCG** (1.0 μM) with the **CA** assembly in 10 mM HEPES buffer at pH 8.0, λ_{ex} = 365 nm. (b) The associated titration curve at λ_{em} = 510 nm and fit according to a 1:1 binding stoichiometry. Data are from n = 3 independent experiments and are presented as mean ± s.e.m..

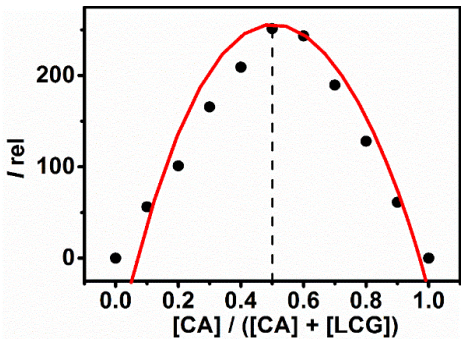

Figure 9. Job's plot for **CA** with **LCG** in 10 mM HEPES buffer at pH 8.0 (λ_{ex} = 365 nm, λ_{em} = 510 nm, [**CA**] + [**LCG**] = 6.0 μM).

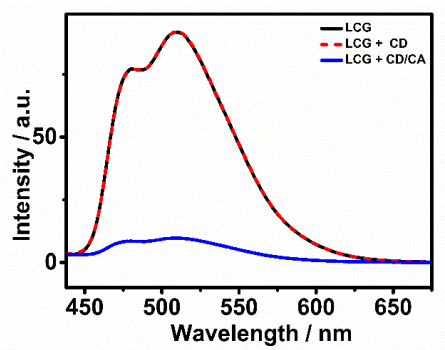

Figure 10. Fluorescence spectra of **LCG** (0.5 μM) and **LCG** (0.5 μM) with the **CD** (2.0 μM) assembly or the **CD–CA** (1.0/1.0 μM) co-assembly in HEPES buffer (10 mM, pH = 8.0, λ_{ex} = 365 nm).

3.2 Binding of calixarene with lysine (K) and arginine (R)

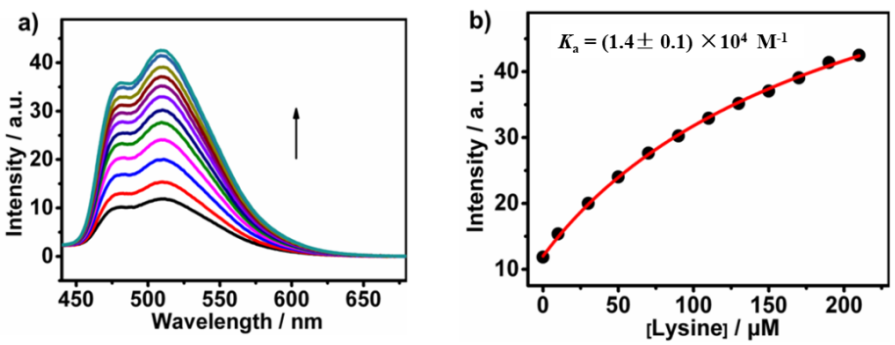

Figure 11. (a) Competitive titration of lysine in the presence of **LCG** (0.5 μM) and the **CA** (1.0 μM) assembly in 10 mM HEPES buffer at pH 8.0 (λ_{ex} = 365 nm), (b) The associated competitive fluorescence titration curve at λ_{em} = 510 nm and fit according to a 1:1 competitive binding model. Data

are from n = 3 independent experiments and are presented as mean ± s.e.m..

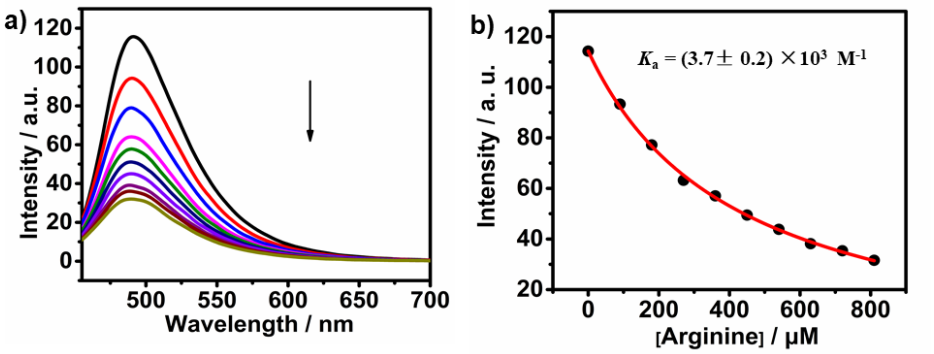

Figure 12. (a) Competitive titration of arginine in the presence of **ThT** (3.0 μM) and the **CD–CA** (5.0/5.0 μM) co-assembly in 10 mM HEPES buffer at pH 8.0 (λ_{ex} = 430 nm), (b) The associated competitive fluorescence titration curve at λ_{em} = 500 nm and fit according to a 1:1 competitive binding model. Data are from n = 3 independent experiments and are presented as mean ± s.e.m.. The association constant between **ThT** and the **CD–CA** co-assembly have been reported previously.[7]

3.3 Binding of model peptides with the CA assembly, CD assembly, CD–CA co-assembly and the simple mixture

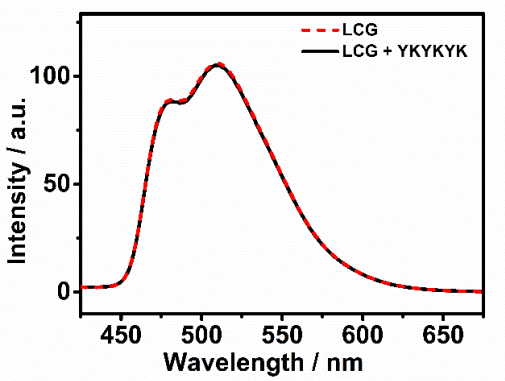

Figure 13. Fluorescence spectra of **LCG** (0.5 μM) and **LCG** (0.5 μM) with **YKYKYK** (50 μM) in HEPES buffer (10 mM, pH = 8.0, λ_{ex} = 365 nm).

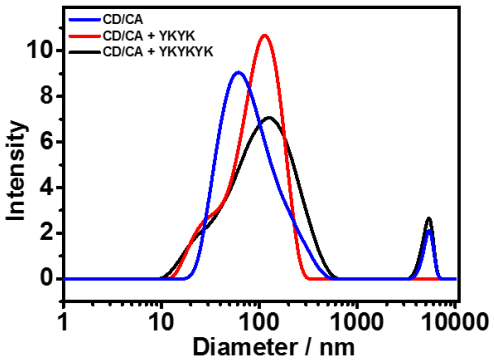

Figure 14. DLS data of the **CD–CA** (1.0/1.0 μM) co-assembly and the **CD–CA** (1.0/1.0 μM) co-assembly with 50 μM **YKYK** or 10 μM **YKYKYK** in HEPES buffer (10 mM, pH = 8.0). Note: there is no aggregate detected in case of 50 μM **YKYK** or 10 μM **YKYKYK** alone.

The model peptides have no appreciable interaction with **LCG** (Supplementary Fig. 13). Slight peak shifts were observed upon addition of **YKYK** and **YKYKYK**, induced by the binding of peptides. However, no extensive cross-linking and aggregation occurred (see previous work on **CD** vesicles aggregation) (Supplementary Fig. 14).[8,9]

The competitive titrations were fitted according to 1:1 binding stoichiometry based on the concentration of **K** unit and obtained binding constants (K_{ave}) express the affinities of one **CA** binding one **K** unit coupled with the synergistic effect of the complexation of **CD** with **Y**.

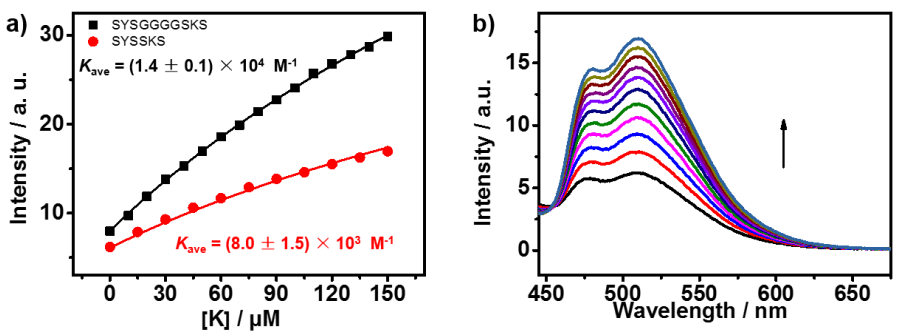

Figure 15. Competitive titration curves of the peptides having different spacer lengths at λ_{em} = 510 nm (a) and competitive fluorescence titration of **SYSSKS** (b) in the presence of **LCG** (0.5 μM) and the

CD–CA (1.0/1.0 μM) co-assembly in 10 mM HEPES buffer at pH 8 (λ_{ex} = 365 nm), fit according to a 1:1 competitive binding model. Data are from n = 3 independent experiments and are presented as mean ± s.e.m..

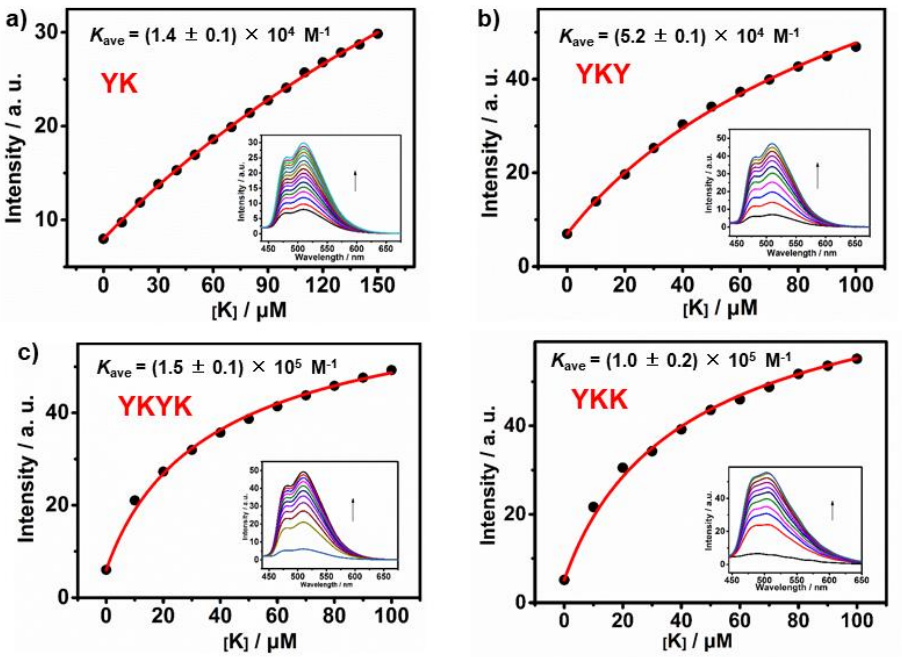

Figure 16. Competitive titration curves of **YK** (a), **YKY** (b), **YKYK** (c) and **YKK** (d) in the presence of **LCG** (0.5 μM) and the **CD–CA** (1.0/1.0 μM) co-assembly in 10 mM HEPES buffer at pH 8.0 (λ_{ex} = 365 nm, λ_{em} = 510 nm), fit according to a 1:1 competitive binding model. Data are from n = 3 independent experiments and are presented as mean ± s.e.m.. Inset: the corresponding competitive fluorescence titrations.

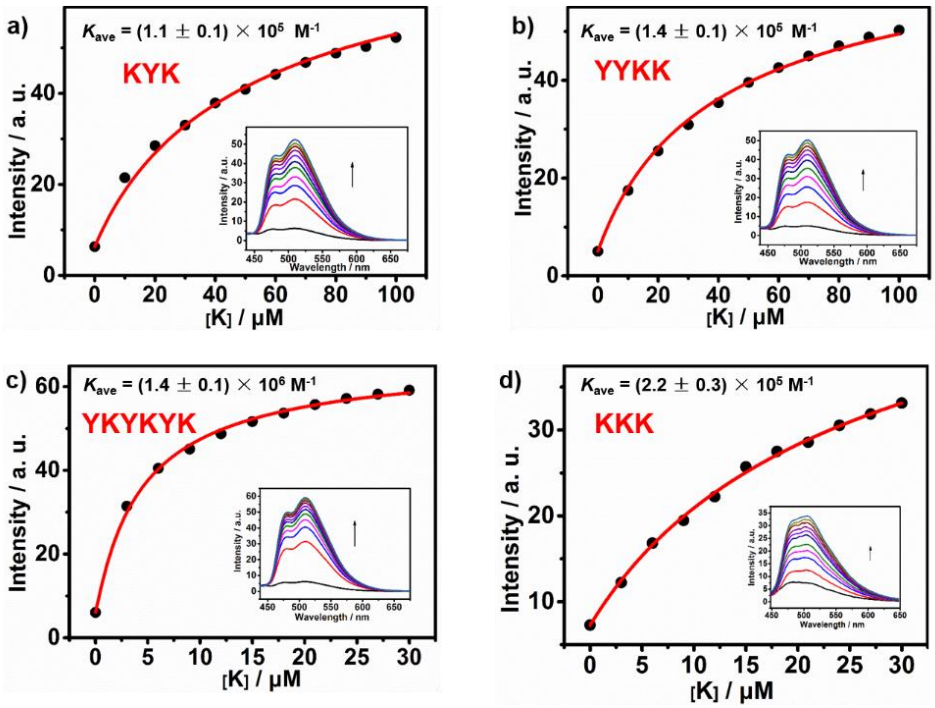

Figure 17. Competitive titration curves of **KYK** (a), **YYKK** (b), **YKYKYK** (c) and **KKK** (d) in the presence of **LCG** (0.5 μM) and the **CD–CA** (1.0/1.0 μM) co-assembly in 10 mM HEPES buffer at pH 8.0 (λ_{ex} = 365 nm, λ_{em} = 510 nm), fit according to a 1:1 competitive binding model. Data are from n = 3 independent experiments and are presented as mean ± s.e.m.. Inset: the corresponding competitive fluorescence titrations.

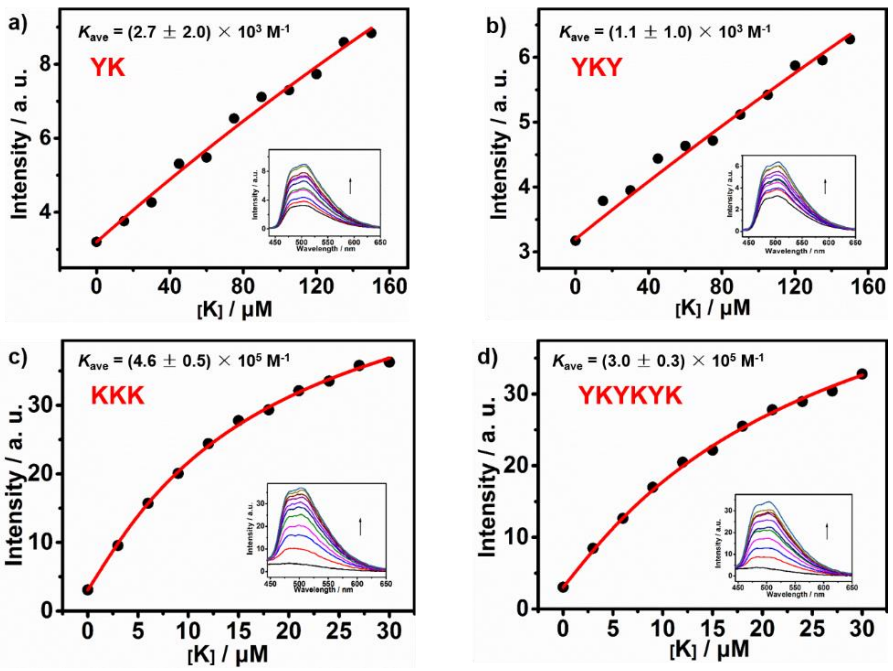

Figure 18. Competitive titration curves of **YK** (a), **YKY** (b), **KKK** (c) and **YKYKYK** (d) in the presence of **LCG** (0.5 μM) and the **CA** (2.0 μM) assembly in 10 mM HEPES buffer at pH 8.0 (λ_{ex} = 365 nm, λ_{em} = 510 nm), fit according to a 1:1 competitive binding model. Data are from n = 3 independent experiments and are presented as mean ± s.e.m.. Inset: the corresponding competitive fluorescence titrations.

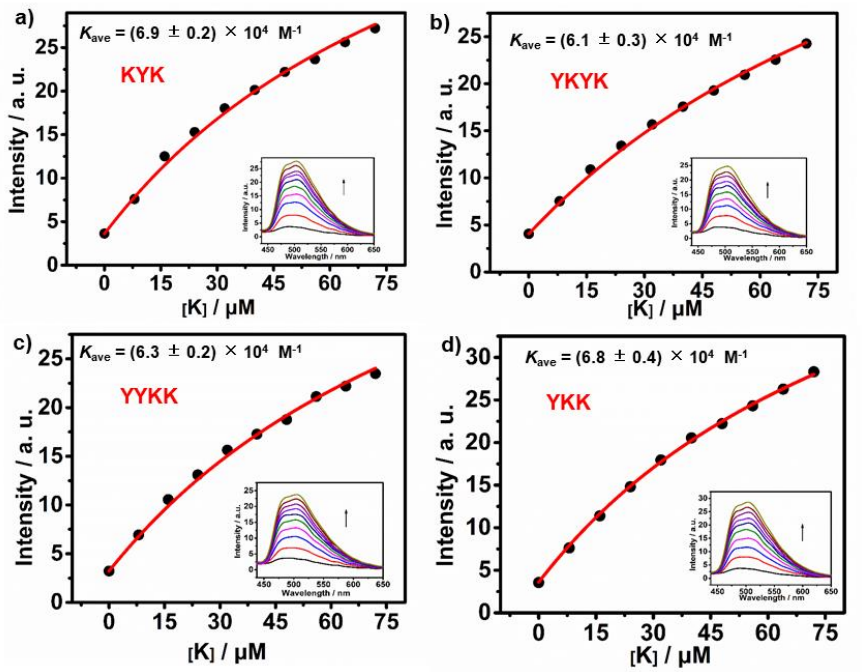

Figure 19. Competitive titration curves of **KYK** (a), **YKYK** (b), **YYKK** (c) and **YKK** (d) in the presence of **LCG** (0.5 μM) and the **CA** (2.0 μM) assembly in 10 mM HEPES buffer at pH 8.0 (λ_{ex} = 365 nm, λ_{em} = 510 nm), fit according to a 1:1 competitive binding model. Data are from n = 3 independent experiments and are presented as mean ± s.e.m.. Inset: the corresponding competitive fluorescence titrations.

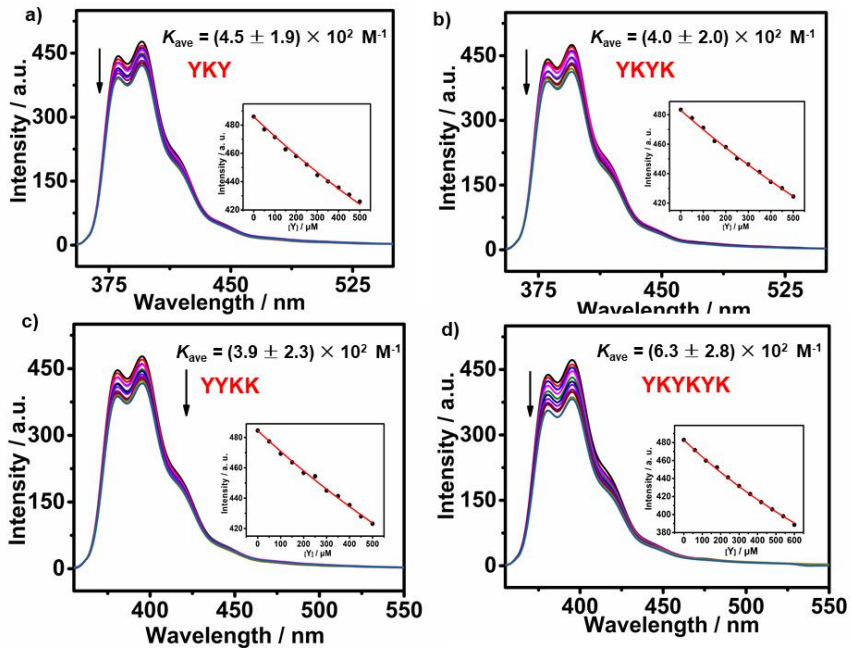

Figure 20. Competitive fluorescence titrations of **YKY** (a), **YKYK** (b), **YYKK** (c) and **YKYKYK** (d) in the presence of **PB** (0.5 μM) and the **CD** (1.0 μM) assembly in 10 mM HEPES buffer at pH 8.0 (λ_{ex} = 326 nm, λ_{em} = 396 nm). Inset: the corresponding competitive titration curves, fit according to a 1:1 competitive binding model. Data are from n = 3 independent experiments and are presented as mean ± s.e.m.. The association constant between **PB** and **CD** has been reported previously.[7]

Table 1 | The association constants (M^{-1}) of model peptides interacting with the **CD** assembly.

	YKY	**YKYK**	**YYKK**	**YKYKYK**
K_{ave}	$(4.5 \pm 1.9) \times 10^{2}$ [§]	$(4.0 \pm 2.0) \times 10^{2}$ [§]	$(3.9 \pm 2.3) \times 10^{2}$ [§]	$(6.3 \pm 2.8) \times 10^{2}$ [§]
K_{multi}	$(2.0 \pm 1.2) \times 10^{5}$ [§]	$(1.6 \pm 1.1) \times 10^{5}$ [§]	$(1.5 \pm 1.3) \times 10^{5}$ [§]	$(2.5 \pm 1.9) \times 10^{8}$ [§]

[§]The competitive fitting gave a fairly big error ascribing to the relatively weak binding and the data are reported only for the information of the reader. Data are from n = 3 independent experiments and are presented as mean ± s.e.m..

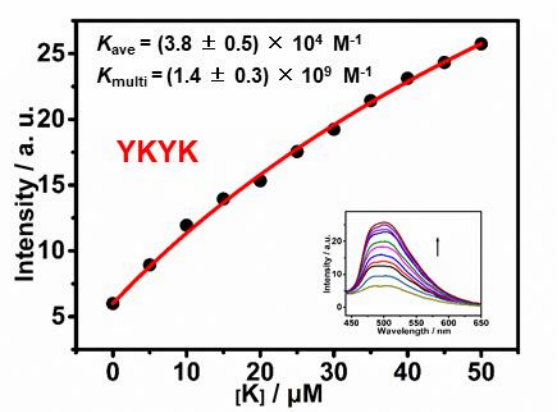

Figure 21. Competitive titration curve of **YKYK** in the presence of **LCG** (0.5 μM) and the **CD** (1.0 μM) assembly simple mixed with **CA** (1.0 μM) assembly in 10 mM HEPES buffer at pH 8.0 (λ_{ex} = 365 nm, λ_{em} = 510 nm), fit according to a 1:1 competitive binding model. Data are from n = 3 independent experiments and are presented as mean ± s.e.m.. Inset: the corresponding competitive fluorescence titrations.

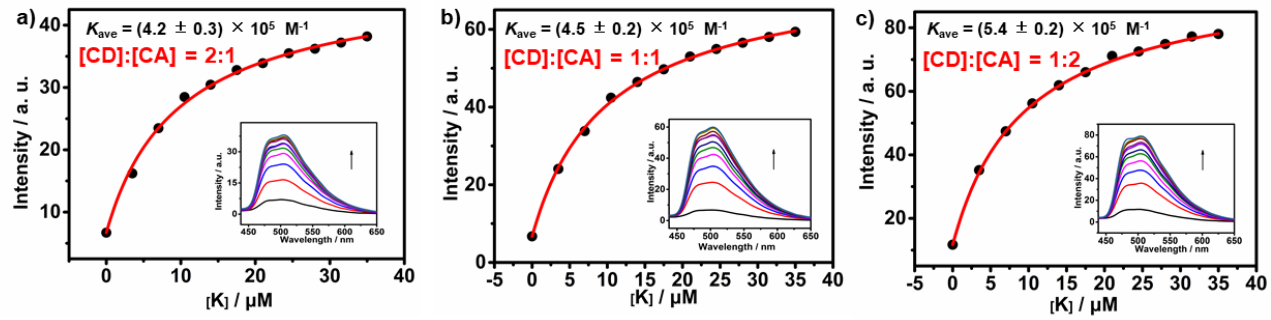

Figure 22. Competitive titration curves of **YKYYKY** in the presence of **LCG** and **CD–CA** co-assemblies having different ratios of **CD** and **CA** in 10 mM HEPES buffer at pH 8.0 (λ_{ex} = 365 nm, λ_{em} = 510 nm, [**CD**]+[**CA**] = 2.0 μM, [**LCG**] = [**CA**]/2), fit according to a 1:1 competitive binding model. Data are from n = 3 independent experiments and are presented as mean ± s.e.m.. Inset: the corresponding competitive fluorescence titrations.

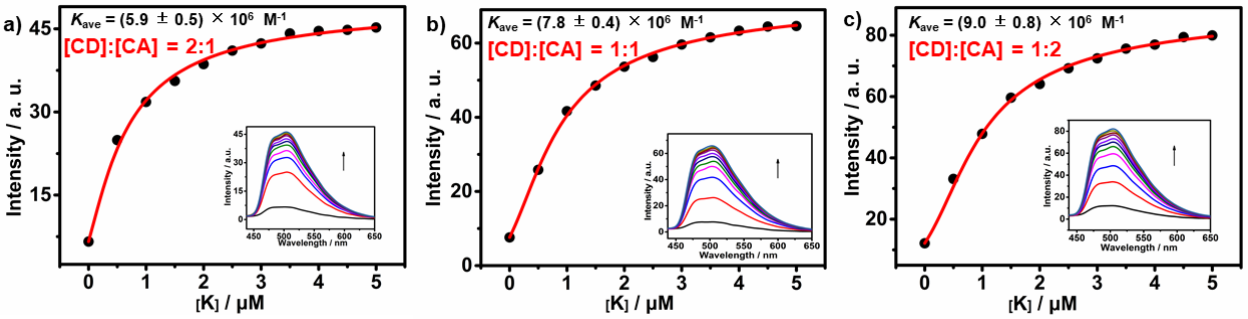

Figure 23. Competitive titration curves of **KYKKYK** in the presence of **LCG** and **CD–CA** co-assemblies having different ratios of **CD** and **CA** in 10 mM HEPES buffer at pH 8.0 (λ_{ex} = 365 nm, λ_{em} = 510 nm, [**CD**]+[**CA**] = 2.0 μM, [**LCG**] = [**CA**]/2), fit according to a 1:1 competitive binding model. Data are from n = 3 independent experiments and are presented as mean ± s.e.m.. Inset: the corresponding competitive fluorescence titrations.

Table 2 | The K_{ave} (M^{-1}) of **YKYYKY** and **KYKKYK** interacting with **CD–CA** co-assemblies prepared at molar ratios of 2:1, 1:1 and 1:2, respectively. (Data are from n = 3 independent experiments and are presented as mean ± s.e.m..)

[**CD**]:[**CA**]	**2:1**	**1:1**	**1:2**
YKYYKY	(4.2 ± 0.3) × 10^5	(4.5 ± 0.2) × 10^5	(5.4 ± 0.2) × 10^5
KYKKYK	(5.9 ± 0.5) × 10^6	(7.8 ± 0.4) × 10^6	(9.0 ± 0.8) × 10^6

4. Characterization of the effects of the CD–CA co-assembly on Aβ_{42}

4.1 Binding between Aβ_{42} and the CD–CA co-assembly

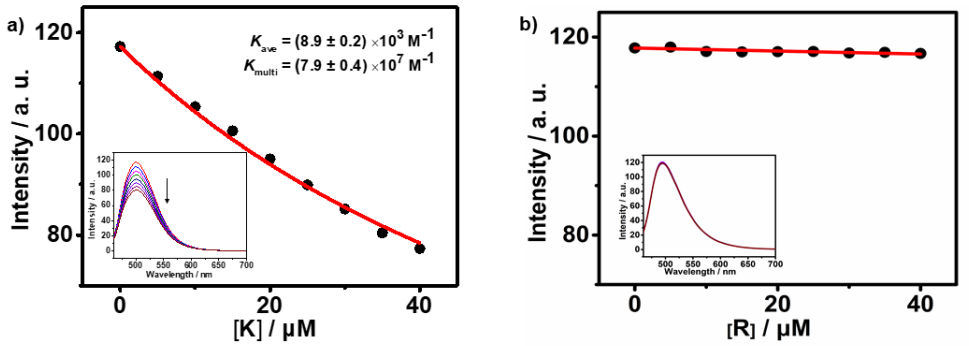

Figure 24. Competitive titration curves of **Aβ_{42}** (a) and **DA-39** (b) in the presence of **ThT** (3.0 μM) and the **CD–CA** (5.0/5.0 μM) co-assembly in 10 mM HEPES buffer at pH 8.0 (λ_{ex} = 430 nm, λ_{em} = 500 nm), fit according to a 1:1 competitive binding model. Data are from n = 3 independent experiments and are presented as mean ± s.e.m.. Inset: the corresponding competitive fluorescence titration. No appreciable change of fluorescence was observed in Supplementary Fig. 24b, indicating no host-guest binding. Note: since **Aβ_{42}** can quench the fluorescence of **LCG**, herein we replaced **LCG** by **ThT** as the reporter dye.

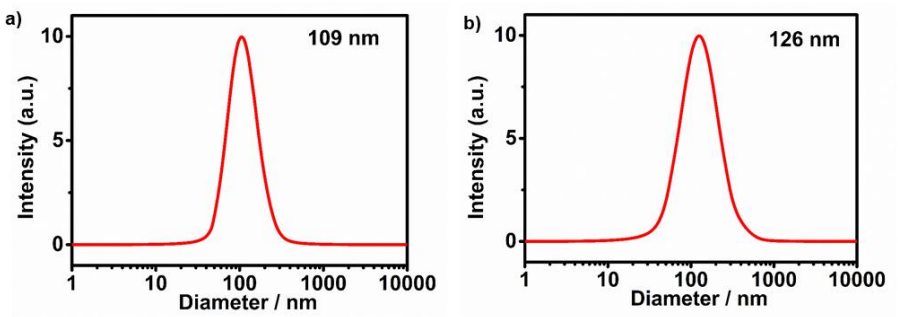

Figure 25. DLS data of (a) the **CD–CA** (50/50 μM) co-assembly and (b) the **CD–CA** (50/50 μM) co-assembly with 50 μM **Aβ_{42}** in 10 mM PBS buffer at pH 7.4.

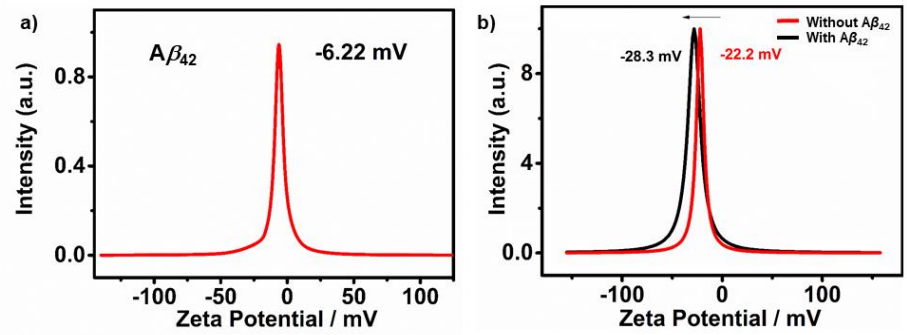

Figure 26. Zeta potentials of (a) 50 μM **A*β*$_{42}$** and (b) the **CD–CA** (50/50 μM) co-assembly with or without 50 μM **A*β*$_{42}$** in 10 mM PBS buffer at pH 7.4.

The results show that in PBS pH 7.4, the size of the **CD–CA** co-assembly became smaller (Supplementary Fig. 25) and the Zeta potential became less negative (Supplementary Fig. 26). Such changes are reasonable since the aggregation of amphiphilic molecules is dependent on the environment. In particular for ionic surfactants, the charge repulsion between ionic heads could be strongly influenced by different buffers and pH values.

4.2 Effects of the CD–CA co-assembly on dissolving A*β*$_{42}$ fibrils

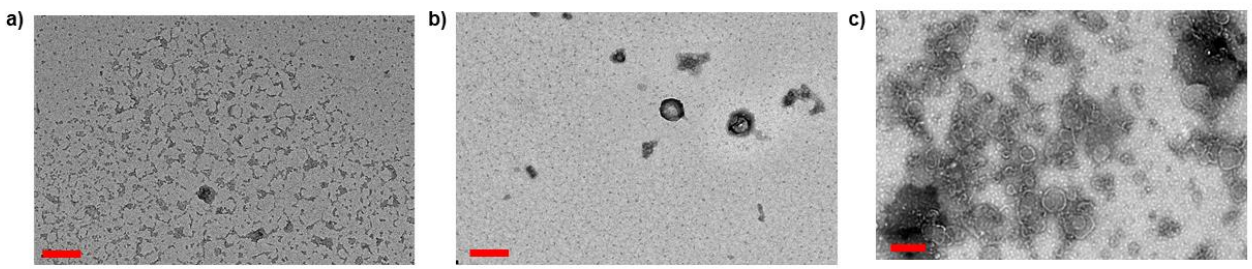

Figure 27. TEM images of (a) fresh 20 μM **A*β*$_{42}$,** (b) the **CD–CA** (20/20 μM) co-assembly and (c) the morphology in sample at 18 h after the **CD–CA** (20/20 μM) co-assembly was added to aggregating solution of 20 μM **A*β*$_{42}$** at 72 h after initiation of aggregation. Scale bar indicates 200 nm. Note: In Supplementary Fig. 27b, the **CD–CA** co-assembly shows hollow spheres with black outlines due to negative staining of tungstophosphoric acid. However, in the presence of **A*β*$_{42}$** (Supplementary Fig. 27c), due to the binding with **CD–CA** co-assembly, tungstophosphoric acid cannot negatively stain and the outline of the hollow sphere becomes white.

5. References

1. Ozawa, R. *et al.* Effect of cyclodextrins on saccharide sensing function of a fluorescent phenylboronic acid in water. *Anal. Sci.* **24,** 207-212 (2008).

2. Xu, Z. *et al.* Broad-spectrum tunable photoluminescent nanomaterials constructed from a modular light-harvesting platform based on macrocyclic amphiphiles. *Adv. Mater.* **28,** 7666-7671 (2016).

3. Falvey, P. *et al.* Bilayer vesicles of amphiphilic cyclodextrins: Host membranes that recognize guest molecules. *Chem. Eur. J.* **11,** 1171-1180 (2005).

4. Mazzaglia, A., Donohue, R., Ravoo, B. J. & Darcy, R. Novel amphiphilic cyclodextrins: graft-synthesis of heptakis(6-alkylthio-6-deoxy)-beta-cyclodextrin 2-oligo(ethylene glycol) conjugates and their omega-halo derivatives. *Eur. J. Org. Chem.* **9,** 1715-1721 (2001).

5. Arena, G., Contino, A., Lombardo, G. G. & Sciotto, D. Water-soluble calix[6]arenes. Characterization of 5,11,17,23,29,35-hexasulphonate-37,38,39,40,41,42-hexahydroxycalix[6]arene and thermodynamic study of proton complex formation. *Thermochim. Acta* **264,** 1-11 (1995).

6. Dos Santos, A. G. *et al.* Changes in membrane biophysical properties induced by the budesonide/hydroxypropyl-β-cyclodextrin complex. *Biochim. Biophys. Acta* **1859,** 1930-1940 (2017).

7. Xu, Z. *et al.* Supramolecular color-tunable photoluminescent materials based on a chromophore cascade as security inks with dual encryption. *Mater. Chem. Front.* **1,** 1847-1852 (2017).

8. Samanta, A., Stuart, M. C. & Ravoo, B. J. Photoresponsive capture and release of lectins in multilamellar complexes. *J. Am. Chem. Soc.* **134**, 19909-19914 (2012).

9. Nalluri, S. K. M., Voskuhl, J., Bultema, J. B., Boekema, E. J. & Ravoo, B. J. Light-responsive capture and release of DNA in a ternary supramolecular complex. *Angew. Chem. Int. Ed.* **50**, 9747-9751 (2011).